

## Coadsorption of K and Cl on the Si(100)(2x1) surface

Shin-ichiro TANAKA, Masao KAMADA and Yukihiro TAGUCHI\*

Institute for Molecular Science, Okazaki 444

\* College of Engineering, University of Osaka Prefecture, Mozu, Sakai, Osaka 591

Coadsorption of K and Cl on the Si(100)(2x1) surface has been studied by the use of core-level photoemission and absorption spectroscopy. All experiments were performed in an UHV chamber equipped with a double-pass CMA, a LEED optics etc, at BL2B1 where the 'grasshopper' monochromator was installed. The sample was a Si(100) wafer ( p-type, B-doped, 10  $\Omega$ cm ). Cleaning was achieved by heating the sample at  $>1350$ K, and was checked by LEED and AES. A commercial getter was used for the evaporation of potassium, and an electrochemical AgCl cell was used for the exposure to chlorine. All spectra were recorded at room temperature. The surface-sensitive absorption spectra were recorded in the Auger electron yield mode with a double-pass CMA, and divided by the photoelectron yield from a gold mesh positioned across the incident light beam in order to eliminate effects due to the transmission function of the monochromator.

Figures 1 show the Si-2p spectra of (a): the clean Si(100) surface, (b): the Si(100) surface covered with a potassium monolayer [ denoted as Si(100)/K hereafter ], (c): the Si(100) surface with a potassium monolayer and subsequently exposed to chlorine [ Si(100)/K/Cl ], and (d): the Si(100) surface exposed to chlorine ( without a potassium layer ) [ Si(100)/Cl ]. The photon energy was 130 eV and the overall resolution was 0.3 eV. It is noted that both coverages of potassium on Si(100)/K and chlorine on Si(100)/Cl are estimated to be 1 according to previous references. Dots are experimental data, lines are least square fits, and dotted lines are backgrounds. Each component has two peaks due to the spin-orbit splitting. All spectra have components at similar binding energies, which are ascribed to the 'bulk' Si atoms (  $Si_{\text{bulk}}$  ). [ Figs. 1(a)-1(d) ] Other components are ascribed to the 'surface' Si atoms, and they have different binding energies and shapes. The components denoted as  $Si_{\text{up}}$  and  $Si_{\text{down}}$  for the clean surface are assigned to the emissions from the upper atoms and the lower atoms, respectively, of the buckled dimers on the reconstructed Si(100)(2x1) surface [ Fig. 1(a) ]. The shift of the binding energies from the

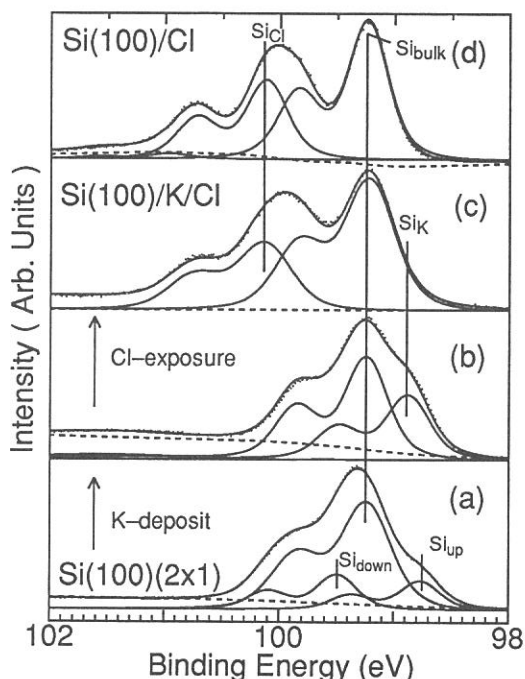


**Figure 1.** Si-2p core-level spectra of (a): clean Si(100)(2x1), (b): Si(100)/K, (c): Si(100)/K/Cl. (d): Si(100)/Cl. Photon energy was 130 eV.

'bulk' components are ascribed to the charge transfer associated with the reconstruction. The  $Si_K$  and  $Si_{Cl}$  components for Si(100)/K and Si(100)/Cl are ascribed to the Si atoms bonded to the potassium and chlorine atoms, respectively [ Figs. 1(b) and 1(d) ]. The shifts of the binding energies for these surface atoms are interpreted to indicate the charge transfer between the substrate atoms ( Si ) and the adsorbate atoms ( K and Cl ), which is caused by their different electronegativity. It is noted that the intensity ratio of the surface components to the bulk components observed for Si(100)/Cl is similar to that for Si(100)/K/Cl. Therefore, the coverage of atoms is estimated to be 1 on Si(100)/K/Cl.

For the Si(100)/K/Cl system, the  $Si_K$  component which is observed for Si(100)/K is extinguished. The binding energy of the surface components for Si(100)/K/Cl is similar to that of  $Si_{Cl}$  component observed for Si(100)/Cl. Thus, it is considered that the configuration of the chemical bond between the Si atom and the Cl atom in the Si(100)/K/Cl system is similar to that in the Si(100)/Cl system, where the atom is bonded to the Si atom via a partially ionized covalent bond.

Figures 2 show K  $L_{2,3}$  core-level absorption spectra of (a): Si(100)/K, (b): Si(100)/K/Cl, and (c): polycrystalline KCl film evaporated on an Au substrate ( recorded in the total electron yield mode ). The splitting of the main two peaks ( 2.8 eV ) observed in all spectra are ascribed to the spin-orbit interaction. These doublets are ascribed to the transition  $2p^6 \rightarrow 2p^5 4s$  and  $2p^6 \rightarrow 2p^5 3d$  ( not resolved ). The peaks observed for Si(100)/K are broad. [ Fig. 2(a) ] It may be related to the metallic character of the Si(100)/K surface and the formation of 4s and 3d bands on the surface. These peaks are sharpened for Si(100)/K/Cl and are very similar to those of the KCl film. This indicates that the chemical nature of K on Si(100)/K/Cl is similar to that in KCl crystal. Thus, it is considered that K is ionized in the Si(100)/K/Cl system.

These results show that Cl atoms are partially ionized and bonded to Si atoms, and K atoms are ionized in the Si(100)/K/Cl system. The coverages of K and Cl are estimated to be 1:1. It is noted that the (2x1) LEED pattern was observed for Si(100)/K/Cl, indicating that there is a ordered structure on this surface. These results are consistent with the other results of the core-level photoemission spectra (  $Cl_{2p}$ ,  $K_{2p}$  and  $K_{3p}$  ), and the Si  $L_{2,3}$  absorption spectra. ( not shown ) Thus, it is concluded that a quasi two-dimensional alkali halide layer is produced on the Si(100)(2x1) surface.

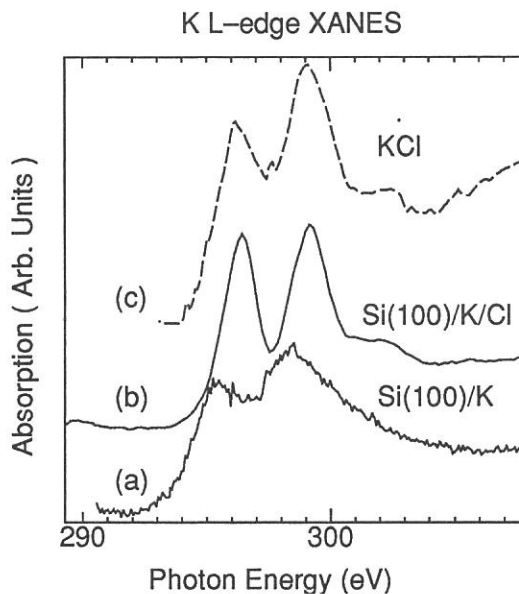


**Figure 2.** Absorption spectra of K- $L_{2,3}$  core levels for (a): Si(100)/K, (b): Si(100)/K/Cl, and (c): KCl film. (a) and (b) were recorded in the Auger electron yield mode, and (c) were recorded in the total electron yield mode.

# DESORPTION OF METASTABLE Ne FROM THE SURFACE OF RARE GAS SOLID BY PHOTON IMPACT

Takato HIRAYAMA\*, Akira Hoshino\*, Daniel E. WEIBEL\*, Ichiro ARAKAWA\* and Makoto SAKURAI\*\*

\*Department of Physics, Gakushuin University, Mejiro, Tokyo 171

\*\*National Institute for Fusion Science, Chikusaku, Nagoya 464

We have studied the desorption of metastable Ne atoms from thin Ne film on solid Ar, Kr, and Xe by photon impact (photon stimulated desorption: PSD) to reveal the mechanism of the desorption induced by electronic transitions (DIET). Experiments have been carried out using a synchrotron radiation at the beam line BL5B in UVSOR, Institute for Molecular Science. Details of the experimental setup and procedure have been previously described.<sup>1</sup>

Kloiber and Zimmerer<sup>2</sup> have proposed two types of models to describe the desorption of excited neutral atoms; "cavity-ejection (CE)" and "excimer-dissociation (ED)" mechanisms. Because the CE process, where the excited atom is desorbed due to the repulsive force from the surrounding atoms in ground state, strongly depends on the electron affinity (EA) of the matrix, the desorption via CE mechanism is expected to take place in solid Ne and Ar (EA < 0), which was experimentally observed<sup>3,4</sup>, but not in solid Kr and Xe (EA > 0). We have investigated the desorption of metastable Ne atoms from thin Ne film on solid Ar, Kr, and Xe to clarify the cavity ejection mechanism.

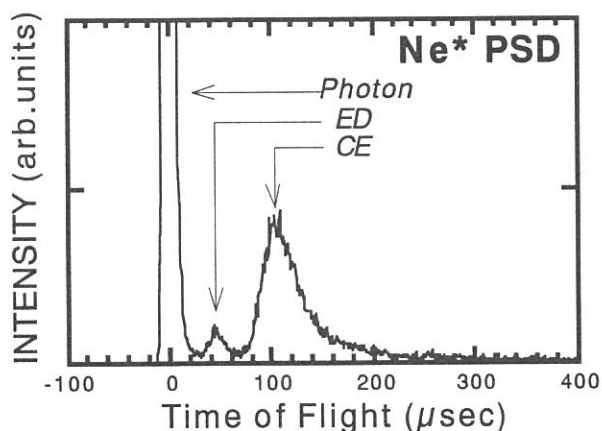


Fig. 1. Typical TOF spectrum of Ne metastables desorbed from solid Ne by photon impact.

Figure 1 shows a typical time-of-flight spectrum of desorbed metastable Ne ( $\text{Ne}^*$ ) from the surface of solid Ne by photon excitation. Two peaks due to the CE and ED mechanisms are clearly shown in the spectrum together with a photon peak, which is used as an origin of the flight time.

Figure 2 shows a dependence of kinetic energies of  $\text{Ne}^*$  desorbed by the CE mechanism on the thickness of the Ne film on solid Ar, Kr, and Xe at the photon energy corresponding to the 1st order surface exciton. The kinetic energies of the Ne metastables are calculated from the flight time and the flight length. The gradual shift of the kinetic energy to the CE peak energy of pure Ne (0.18 eV) shows that  $\text{Ne}^*$  in the Kr and Xe matrix, whose electron affinities are positive, can desorb from the surface via the CE mechanism.

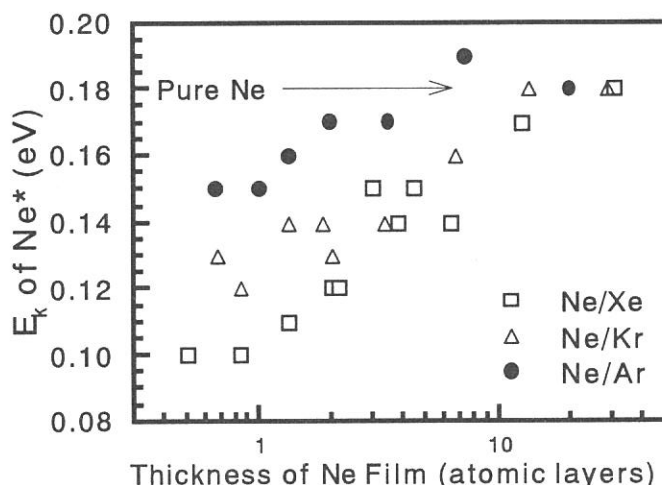


Fig.2. Dependence of kinetic energies of  $\text{Ne}^*$  desorbed through the CE mechanism on the thickness of a Ne film on solid Ar, Kr, and Xe.

## REFERENCES

- <sup>1</sup>M. Sakurai, T. Hirayama, and I. Arakawa, *Hosyakou* **5**, (1992) 13. (in Japanese): M. Sakurai, T. Hirayama and I. Arakawa, *Vacuum* **41**, (1990) 217.
- <sup>2</sup>T. Kloiber and G. Zimmerer, *Rad. Eff. Def. Sol.* **109**, 219 (1988).
- <sup>3</sup>F. Colletti, J. M. Debener, and G. Zimmerer, *J. Phys. (Paris) Lett.* **45**, L467 (1984); T. Kloiber and G. Zimmerer, *Physica Scripta* **41**, 962 (1990).
- <sup>4</sup>I. Arakawa, M. Takahashi, and K. Takeuchi, *J. Vac. Sci. Technol. A* **7**, 2090 (1989); D. J. O'Shaughnessy, J. W. Boring, S. Cui, and R. E. Johnson, *Phys. Rev. Lett.* **61**, 1635 (1988)

## Time Response of Excited-State Na Desorption from SR-Irradiated Na-Halides

Sayumi Hirose and Masao Kamada

Institute for Molecular Science, Myodaiji, Okazaki 444

Bombardment of solids by energetic electron- or photon-beams causes the ejection of constituent species from the surface. There are numerous studies of the electron-stimulated desorption (ESD) from alkali halides. However few groups have studied the photon-stimulated desorption (PSD) of excited species.<sup>1)</sup> The purpose of present study is to get a better understanding of the PSD mechanism. Time response of excited-state Na desorption from SR-irradiated Na-halides has been investigated by using a method of time-correlated single photon counting.

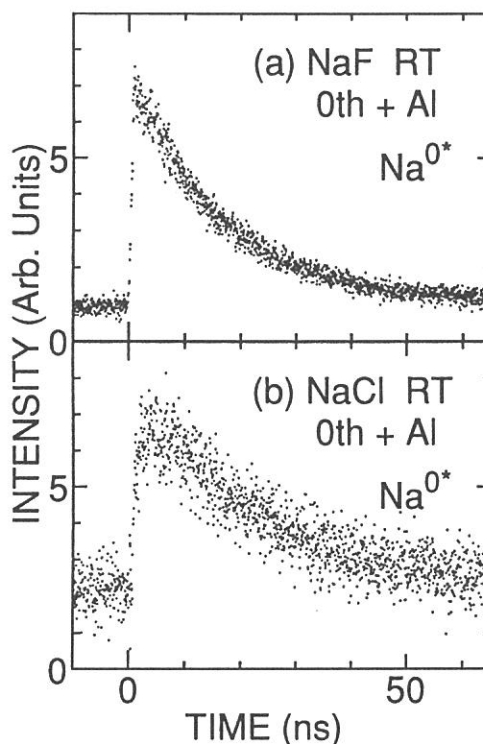
Experiments were performed at a PGM beam line 6A2. The interval of successive SR pulses was 178 ns and the full-width at half-maximum of a bunch was 500 ps. Time response measurements were carried out with a time-correlated single photon counting method. Single crystals were cleaved with a knife edge in sample chamber and were excited with the zeroth-order light through the aluminum film.

Emission spectra of Na halides are composed of the atomic emission (so-called Na D-line) at about 2.1 eV due to the transition from desorbed excited-state Na atoms and broad bands.<sup>2)</sup> Therefore, in order to obtain the time response of the excited-state Na desorption, atomic line was separated from the broad band with using the time response data observed at 2.07, 2.10 and 2.14 eV. The results obtained after the separation are shown in figure 1. These time responses are composed of fast and slow components. The fast component is in the time scale of nano-second and the slow component is between 178 ns and 3 ms. The slowest limit was determined with the mechanical chopper method. The time response of ground-state Na atoms has been regarded to be in the scale of  $\mu$ s to ms by Kanzaki et al.<sup>3)</sup> and Loubriel et al.<sup>4)</sup>. Kanzaki et al.<sup>3)</sup> have observed the decay time and the temperature dependence of PSD of neutrals from alkali halides, and proposed that the desorption process of ground-state alkali atoms is related to the diffusion of Vk centers and the surface reaction of F centers and alkali ions. Loubriel et al.<sup>4)</sup> have studied the time dependence of ESD of ground-state Li from LiF, and explained the persistence of the Li emission in terms of the slow diffusion of bulk F centers. From the comparison between the time response of excited- and ground-state alkali desorption, the slow component of excited-state alkali desorption is seemed to be

in the time scale of ground-state alkali desorption. Therefore, the slow desorption of excited-state alkali atoms may be due to the same mechanism as that of ground-state alkali atoms. On the other hand, the fast component of excited-state alkali desorption is in the time scale of nano-second, and so the fast desorption may be related to the lattice defect formation (for example STE, F-H pair formation, and so on) due to the electronic excitation in the surface layer and the charge transfer to alkali ions.

It should be noted that the time response of NaF (Fig. 1a) is much different from that of NaCl (Fig. 1b). That is, the ratio of fast and slow components is about 1.5 and 3 for NaF and NaCl, respectively. The decay time of fast component of NaCl is 1.2 times larger than that of NaF. These differences may be related with the substance dependence reported previously.<sup>2)</sup>

Fig.1 Time response of excited-state Na atom desorption from NaF (a) and NaCl (b) excited with the zeroth-order light through the aluminum film at room temperature.



#### References

- 1) Desorption Induced by Electronic Transitions (DIET IV), edited by G. Betz and P. Varga (Springer, Berlin, 1990).
- 2) S. Hirose and M. Kamada, J. Phy. Soc. Jpn., 60, 4376, (1991)
- 3) H. Kanzaki and T. Mori, Phys. Rev. B29, 3573 (1984)
- 4) G. M. Loubriel, T. A. Green, N. H. Tolk and R. F. Haglund, Jr., J. Vac. Sci. Technol. B5, 1514 (1987)

# THERMAL AND PHOTODECOMPOSITION OF IRON PENTACARBONYL ADSORBED ON TITANIUM AND OXIDIZED TITANIUM SURFACES

Masahiko MOROOKA\*, Sadao HASEGAWA\*, Tadashi HASEGAWA\*, Shosuke  
TERATANI\*, Shinri SATO\*\*, and Yuji UKISU\*\*

\**Department of Chemistry, Tokyo Gakugei University, Koganei, Tokyo 184, Japan*

\*\**Institute for Molecular Science, Myodaiji, Okazaki 444, Japan*

Irradiation of iron pentacarbonyl,  $\text{Fe}(\text{CO})_5$ , adsorbed on solid surfaces leads to formation of a variety of products depending on the type of surface.<sup>1)</sup> On insulator surfaces, a dimer or a trimer of  $\text{Fe}(\text{CO})_5$  is formed depending on acid-base property of the surface, while complete photodecomposition occurs at room temperature on semiconductor or metal surfaces.<sup>1)</sup> To study a detailed mechanism of the photolysis of  $\text{Fe}(\text{CO})_5$  adsorbed on metal surfaces, a reaction intermediate has been investigated by a low-temperature adsorption method using IR reflection absorption spectroscopy (IRAS), X-ray photoelectron spectroscopy (XPS), and temperature programmed desorption (TPD) technique.

In the present study a Ti polycrystal plate was used as a substrate. Since Ti oxides show the property of semiconductor, the Ti sample was oxidized in oxygen at 1000K and then used as another substrate to examine a difference in a reaction mechanism between metal and semiconductor surfaces. All the experiments were conducted in the UHV chamber of BL-4A, which had been constructed for the study of surface photochemistry<sup>2)</sup>. Because surface impurities give crucial effects on the adsorption state of  $\text{Fe}(\text{CO})_5$ , the sample surface was cleaned by repeating Ar ion sputtering at 673K for 1 hr followed by annealing at 900K for 5 min. SOR light was passed through a sapphire filter which cutoff wavelength is ca. 150 nm. The coverage of  $\text{Fe}(\text{CO})_5$  on the surface is about monolayer unless otherwise stated.

It is very important to examine adsorption states of reactants in surface photochemistry, since electronic states as well as geometrical structure of adsorbed molecules are often quite different from those observed in the gas phase. Fig. 1 shows the  $\text{C}_{1s}$  XPS spectra of  $\text{Fe}(\text{CO})_5$  adsorbed on a clean Ti surface at 100K: The peaks at the binding energies of 282, 286, and 288eV are assigned to the carbons of carbide, carbonyl in subcarbonyl species, and carbonyl in  $\text{Fe}(\text{CO})_5$ , respectively.<sup>3)</sup> This result indicates that  $\text{Fe}(\text{CO})_5$  adsorbed directly on Ti undergoes thermal decomposition even at 100K to form partially decarbonylated species,  $\text{Fe}(\text{CO})_{5-x}$  ( $x = 1 - 4$ ), and carbide. The formation of carbide implies thermal dissociation of CO released from  $\text{Fe}(\text{CO})_5$  and therefore remarkable reactivity of a Ti surface. Fig. 1 also shows temperature dependence of the  $\text{C}_{1s}$  spectrum; adsorbed  $\text{Fe}(\text{CO})_5$  decomposes further with rise in temperature. Fig. 2 shows the thermal desorption spectra recorded after the adsorption of  $\text{Fe}(\text{CO})_5$  on the clean Ti sample. The solid line denotes  $\text{CO}^+$  produced from  $\text{Fe}(\text{CO})_5$  and CO in a quadrupole mass spectrometer, and the dotted line  $\text{Fe}^+$  exclusively from  $\text{Fe}(\text{CO})_5$ . The peaks below 120K is due to the desorption from a heater of the sample holder. Because these spectra involve contribution from the back of sample, which was not cleaned by Ar ion sputtering, the desorption peak of  $\text{Fe}(\text{CO})_5$  at ca. 150K is attributable to the

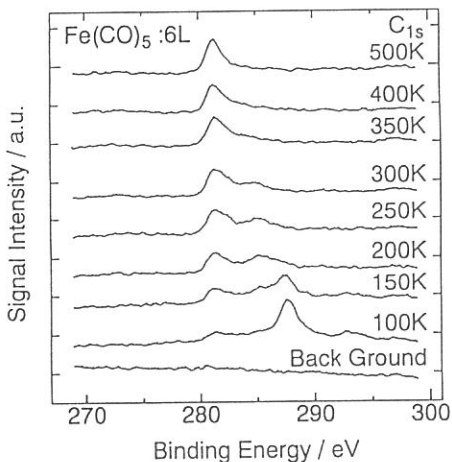


Fig. 1. C1s XPS spectra of  $\text{Fe}(\text{CO})_5$  adsorbed on the Ti sample.

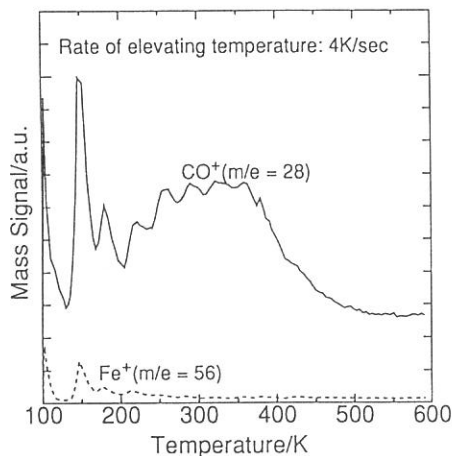


Fig. 2. Thermal desorption spectra of  $\text{Fe}(\text{CO})_5$  adsorbed on the Ti sample.

uncleaned surface, on which  $\text{Fe}(\text{CO})_5$  physisorbs. The  $\text{Fe}(\text{CO})_5$  desorption peak at ca. 180K is ascribable to physisorbed  $\text{Fe}(\text{CO})_5$  which may exist on a carbided surface produced by thermal dissociation of carbonyl. The multiple desorption peaks of CO at temperatures above 200K arise from decomposition of decarbonylated (intermediate) species, and suggest that various states of the intermediate species are yielded. The IRAS spectrum of adsorbed  $\text{Fe}(\text{CO})_5$  (not shown here) exhibits a single CO stretching band, suggesting that a trigonal-bipyramidal form in the gas phase is changed to a square pyramidal form on the surface, and the broad shoulder in lower frequencies is indicative of the presence of decarbonylated species. With rise in temperature the main band assignable to physisorbed  $\text{Fe}(\text{CO})_5$  disappears below 180K in agreement with the result of TPD.

Irradiation of the adsorbed  $\text{Fe}(\text{CO})_5$  with SOR (>150 nm) light leads to evolution of CO, but no photodesorption of  $\text{Fe}(\text{CO})_5$  was observed. XPS, IRAS, and TPD spectra show that physisorbed  $\text{Fe}(\text{CO})_5$  rapidly undergoes photo-decarbonylation to form partially decarbonylated intermediate. When the substrate is heated, the intermediate species shows similar behaviors to the thermally decarbonylated species. Neither composition nor geometry of the photo-product, however, has been determined since the decarbonylated species produced by thermal decomposition already presents too much on the surface. To avoid the thermal decomposition of  $\text{Fe}(\text{CO})_5$ , the Ti sample was oxidized. After the oxidation, TPD analysis shows that the thermal decarbonylation is greatly suppressed, while IRAS indicates that the adsorption state of  $\text{Fe}(\text{CO})_5$  is quite different from that observed for metal surfaces. Further investigation is under progress.

## References

- 1) S. Sato, Hyomen Kagaku, **13**, 225(1992).
- 2) S. Sato, Y. Ukisu, E. Nakamura, T. Kinoshita, A. Hiraya, and M. Watanabe, UVSOR Report 11(1991).
- 3) S. Sato and Y. Ukisu, Surf. Sci., in press.



## Photodecomposition of Iron Pentacarbonyl Adsorbed on Silver Surfaces

Yuji UKISU, Hisashi OGAWA, and Shinri SATO  
Institute for Molecular Science, Myodaiji, Okazaki 444, Japan

Surface photochemistry of organometallic compounds has received increasing attention because of its application to production of a variety of functional materials. For a deeper understanding of a mechanism of surface photochemical reactions, information on structure and geometry of adsorbed molecules becomes indispensable. This paper reports observation of the photolysis of iron pentacarbonyl adsorbed on silver surfaces using IR reflection absorption spectroscopy (IRAS), temperature-programmed desorption (TPD) technique and X-ray photoelectron spectroscopy (XPS).

Experiments were done with a UHV chamber at BL-4A.<sup>1)</sup> Silver samples used were a polycrystalline plate and cleaned by Ar ion sputtering. Monolayer coverage was achieved by 6-8 L dosing of  $\text{Fe}(\text{CO})_5$  (L = Langmuir,  $10^{-6}$  torr/sec). SOR light was irradiated to the sample through a sapphire or glass cutoff filter.

Figure 1 shows the IRAS spectra of  $\text{Fe}(\text{CO})_5$  adsorbed on Ag surface at 100 K before and after irradiation of SOR (>150 nm) light at different coverages. In the spectrum after irradiation at coverages below monolayer, a new C-O stretching band due to subcarbonyl species assignable to  $\text{Fe}(\text{CO})_4$  or  $\text{Fe}(\text{CO})_3$  is observed at lower frequencies. In multilayer  $\text{Fe}(\text{CO})_5$ , the photolysis leads to appearance of a broad band at higher frequencies, indicating formation of oligomers such as  $\text{Fe}_2(\text{CO})_9$  and  $\text{Fe}_3(\text{CO})_{12}$ .

Figure 2 shows TPD spectra of  $\text{CO}^+$  ( $m/e=28$ ) before and after the photolysis. A desorption peak at around 180 K is due to the desorption of physisorbed  $\text{Fe}(\text{CO})_5$  in multilayer and peaks above 200 K are attributable to the thermal decarbonylation of adsorbed species bound strongly to the surface and photoproducts. The average composition of photoproducts can be estimated from a change in peak areas between the low and high temperature peaks, and the result shows that the CO/Fe ratio is about 4 at nearly monolayer coverage and decreases to less than 3 with further increase in coverage, indicating the extent of photo-decarbonylation depends upon coverages.

XPS spectra of  $C_{1s}$ ,  $O_{1s}$  and  $Fe_{2p}$  (Fig.3) show that their binding energies shift to lower energies after irradiation. This indicates again formation of subcarbonyl species. From the comparison of peak areas of  $C_{1s}$  and  $Fe_{2p}$ , the photoproduct is assumed to be  $Fe(CO)_4$ . After heating up to 330 K, C and O signals disappear and deposition of Fe metal is observed.

We conclude that an intermediate of the photolysis is  $Fe(CO)_4$  stabilized due to strong interaction between the carbonyl ligands and the surface, and the intermediate undergoes further photo-decarbonylation to form oligomers at multilayer coverages.

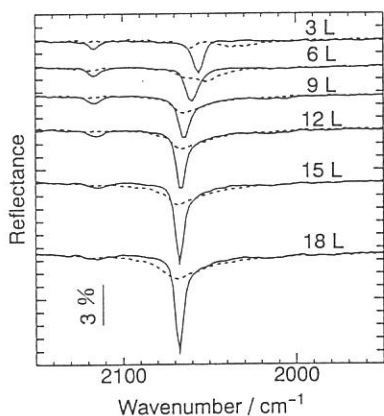


Fig.1. IRAS spectra of  $Fe(CO)_5$  adsorbed on Ag at different coverages before (solid line) and after (dotted line) irradiation ( $>150$  nm) for 10 min.

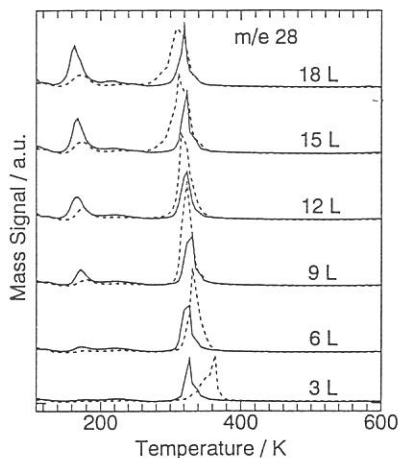


Fig.2. TPD spectra of  $CO^+$  ( $m/e=28$ ) from  $Fe(CO)_5$  adsorbed on Ag at different coverages before (solid line) and after (dotted line) irradiation ( $>150$  nm) for 10 min.

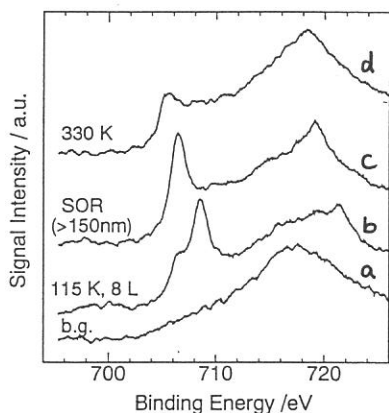


Fig.3. XPS  $Fe_{2p}$  spectra of  $Fe(CO)_5$  adsorbed on Ag; (a) before adsorption; (b) after 8 L dosing; (c) after irradiation ( $>150$  nm) for 30 min; (d) after heating to  $>330$  K.

#### References

- 1) S.Sato, Y.Ukisu, E.Nakamura, T.Kinoshita, A.Hiraya, and M.Watanabe, UVSOR Activity Report, p.11 (1991).

# SYNCHROTRON RADIATION EXCITED ETCHING OF SILICON SURFACE STUDIED BY VELOCITY DISTRIBUTION MEASUREMENTS OF DESORBED SPECIES

Haruhiko OHASHI, Kiyohiko TABAYASHI and Kosuke SHOBATAKE

*Institute for Molecular Science, Myodaiji, Okazaki 444, Japan*

The neutral species desorbed from the surface in the etching reaction of crystalline Si(100) have been identified from the measurements of their velocity distributions using a time-of-flight (TOF) technique combined with an electron bombardment ionization mass spectrometry. The preliminary measurements of the velocity distributions indicate that the desorbed species formed in the etching reactions of Si with XeF<sub>2</sub> are essentially identical for the undulator on and off although irradiation of synchrotron radiation (SR) promotes the etching reaction.

In the present study very reactive etchant XeF<sub>2</sub> gas was used to avoid the etchant gas pressure to exceed  $1.0 \times 10^{-4}$  Torr in the reaction chamber and yet to supply enough F atoms to the surface. The schematics of the apparatus is shown in Fig. 1.

The reaction chamber is connected to the undulator beam line BL3A1. The gap length of the undulator magnets was 60 mm where the peak energy of the 1st order light is 35.8 eV. The incident angle of the undulator light was 75 degrees and the species desorbing into the direction of 15 degrees were monitored. The undulator beam is perpendicular to the axis of quadrupole mass filter.

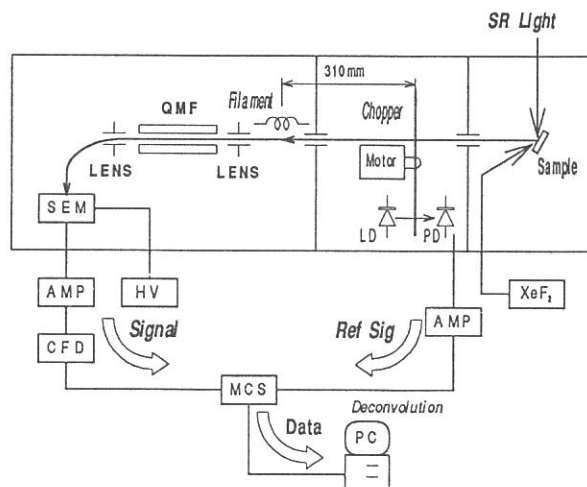


Fig.1 Schematic of the apparatus for the measurements of the velocity distributions of the desorbed species formed in the etching reaction of SiO<sub>2</sub> and Si with XeF<sub>2</sub>.

The desorbed species enters the chopper chamber through an aperture. A molecular beam of the desorbed species which is modulated with a correlation copper enters the mass spectrometer chamber. The beam molecules are

detected by an electron bombardment ionization quadrupole mass spectrometer. Since the ion energy is much larger than the thermal translational energy of the neutral species, the time spent from the moment of a neutral species passing the chopper to that of ion detection is essentially equal to the neutral flight time (from the chopper to the ionizer). The flight length from the chopper to the ionizer was 31.0cm.

The velocity distributions of the desorbed species from the substrate surface were measured at masses  $m/e = 47, 66, 75,$  and  $85$  with the undulator beam on and off. From the TOF distributions of the desorbed species we conclude that the only products with relatively heavy masses  $M > 100$  are desorbed. The typical TOF spectra measured at ion mass  $m/e = 85$  ( $\text{SiF}_3^+$ ) with SR on and off are illustrated in Fig. 2. The substrate was kept at room temperature ( $27^\circ\text{C}$ ) and the  $\text{XeF}_2$  pressure was at  $1.1 \times 10^{-5}$  Torr. The solid lines are the calculated Maxwell-Boltzmann distributions with a functional form in the time space for the neutral flight time  $t = L/v$ :

$$F(t) \propto \left(\frac{v}{\alpha}\right)^4 \exp\left(-\left(\frac{v}{\alpha}\right)^2\right)$$

where  $\alpha$  is the most probable velocity  $\alpha = \{2RT/M\}^{1/2}$  for translational temperature  $T = 300$  K and a neutral mass  $M =$

104 which corresponds to  $\text{SiF}_4$ . If a mass of the desorbed species  $M = 85$  ( $\text{SiF}_3$ ) is assumed the calculated distribution does not fit well to the observed one. From the results mentioned above we conclude that the parent molecule detected at  $m/e = 85$  is not  $\text{SiF}_3$  but  $\text{SiF}_4$  even for the beam on. This is an important observation since the species desorbed from the surface on a repulsive potential energy surface or kept at a higher temperatures than room temperature just after photoexcitation, can exhibit a velocity distribution for  $T$  higher than the room temperature. In fact from Fig. 2 one finds that 1) the distributions for the beam on and off are basically identical with each other except for the higher intensity for the SR beam on, and 2) the product intensity is higher for the SR beam on than for the beam off within the experimental error.

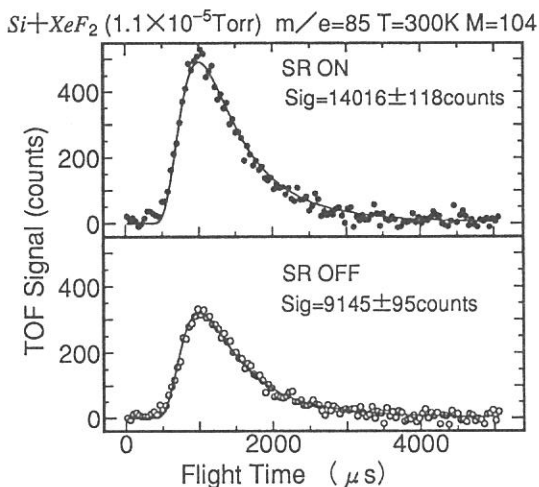


Fig.2 TOF spectra of desorbed species detected at mass  $m/e = 85$  with SR beam on and off. The solid curves corresponds to calculated Maxwellian for mass  $M = 104$ .

## Synchrotron radiation assisted epitaxial growth of compound semiconductor using metalorganic sources

Hiroshi OGAWA, Mitsuhiro NISHIO, Makoto IKEJIRI,  
Toshihiro OGATA, and Akira YOSHIDA\*

Department of Electronic Engineering, Faculty of Science and  
Engineering, Saga University, 1 Honjo, Saga 840, Japan

\*Institute for Molecular Science, Myodaiji, Okazaki 444, Japan

The synchrotron radiation (SR) seems to provide a new light source in low-temperature growth process. In order to demonstrate its usefulness, we have investigated the growth of ZnTe, which is a II-VI compound semiconductor. In this report, we describe the first successful growth of compound semiconductor using metalorganic sources by the SR irradiation.

The apparatus used in the present experiment is illustrated schematically in fig. 1. This apparatus was connected with the differential pumping chamber system in the beam line BL-8A of UVSOR facility at Institute for Molecular Science. Diethylzinc and diethyltelluride were used as source materials. As a carrier gas, hydrogen was employed. The substrate was (100) oriented GaAs. The growth was carried out in the same manner as previously reported<sup>1)</sup> except that the substrate holder was not heated. That is, the introduction of source gases into the chamber, formation of adsorbed layer and decomposition of adsorbed source molecules by the SR irradiation (one cycle for growth) were repeated.

Figure 2 shows the microphotograph of the film deposited on the substrate and the corresponding result measured with a surface-roughness meter. The film has a relatively smooth and featureless surface morphology. The boundary between the film is estimated to be 1000 to 1500 Å. This value corresponds to 5 to 8 Å/cycle in average, implying the surprising slow growth of atomic layer order.

Both the Zn 2p core level XPS signal and the Te 3d signal were distinctly observed in the grown layer, showing that the film is ZnTe.

Until the growth exceeds 15 cycles, the RHEED pattern of the film exhibits streak pattern. The pattern changes to the spotty one after 15 cycles and then retains it through the experiment. Figure 3 shows the RHEED pattern (20 keV, [011] azimuth) of ZnTe film on (100) GaAs substrate when the number of growth cycles is 190. The distinct and clear spot pattern clearly shows the single crystalline film and excellent crystallinity. Furthermore, as shown in fig. 3b, the array of diffraction spots confirms the epitaxial layer.

The substrate temperature rise due to the SR irradiation itself is probably negligible because of the use of low power less than 0.3W and

the intermittent introduction of SR light. Hence, it can be concluded that the SR irradiation offers the epitaxial growth at room or low temperature using metalorganic sources.

1) H. Ogawa, M. Nishio and M. Ikejiri, UVSOR activity report (1992).

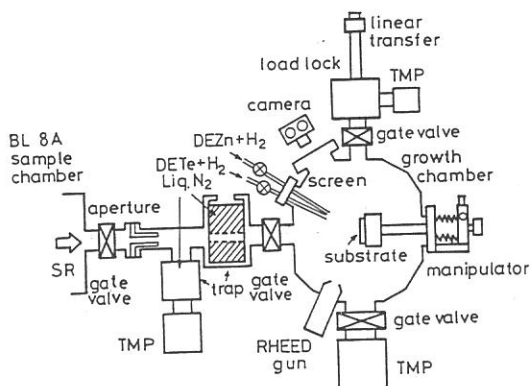


Fig. 1. Schematical experimental apparatus.

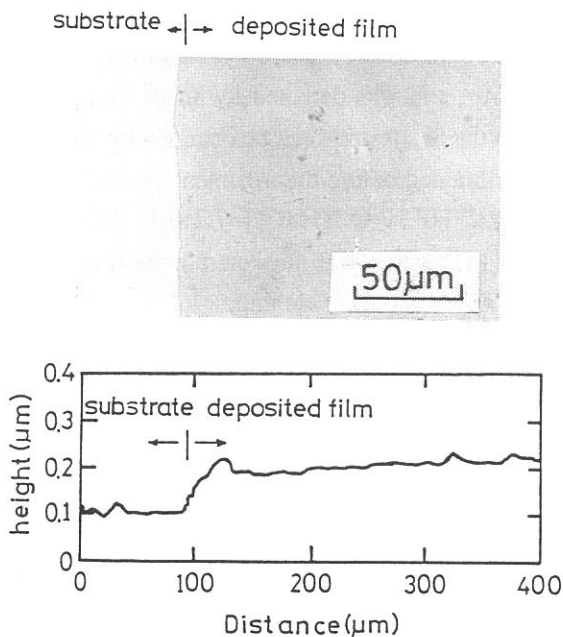


Fig. 2. The microphotograph of the film deposited on the substrate and the result measured with surface roughness meter.

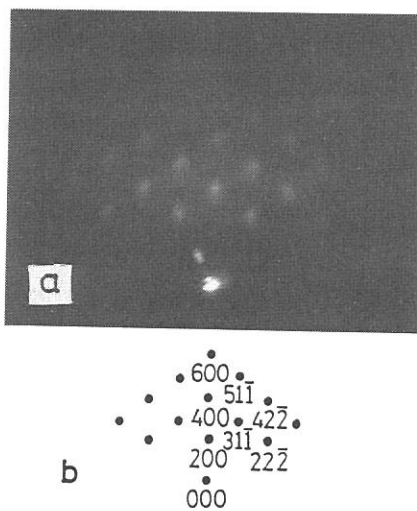


Fig. 3. A typical RHEED pattern of the deposited film (a), and the array of the diffraction spots expected for ZnTe crystal with an (100) surface (b).

# OPTICAL CHARACTERIZATION OF Si SURFACE BY HIGH-SENSITIVITY INFRARED REFLECTANCE SPECTROSCOPY

Masanori OKUYAMA, Masahiro NISHIDA, Junko IZUMITANI, Takeshi KANASHIMA

*Department of Electrical Engineering, Faculty of Engineering  
Science, Osaka University, Toyonaka, Osaka 560, Japan*

Atomic bondings and morphology on the Si surface have attracted much attention with respect of microfabrication of Si integrated devices, because Si atomic layer steps and/or oxide on the Si surface change the electrical properties of the prepared Si or SiO<sub>2</sub> film, and affect basic characteristics of the fabricated devices. High-sensitivity infrared reflection spectroscopy has a sufficient sensitivity to give detailed information about the chemical state of the substrate and deposited film during in-situ deposition. We investigated Si(111) surface in-situ using high-sensitivity infrared reflection spectroscopy, and studied the surface reaction and atomic condition of Si treated with O<sub>2</sub> or H<sub>2</sub> gas and wet etching with and without irradiation in a vacuum chamber.<sup>1)</sup>

A Si wafer of 4-inch diameter was supported in a vacuum chamber of 500 mm  $\phi$  diameter and 400 mm length. An infrared beam from a fourier-transformation infrared (FT-IR) spectrometer was concentrated by a concave mirror and applied to the Si wafer through a window plate in a vacuum chamber. The reflected infrared beam exited through the other window, was concentrated by a focusing mirror, and was detected by an IR detector. The absorption induced by species and molecules on the Si substrate can be obtained by dividing the spectrum measured after the treatment by that obtained before the treatment. A Si(111) wafer was etched with 5% HF solution or BHF(NH<sub>4</sub>F:HF:H<sub>2</sub>O:NH<sub>4</sub>OH=7:1:6:1) solution after RCA cleaning. Reflectance spectrum of the Si(111) wafer was measured in the film treated at 200°C in 5Torr O<sub>2</sub> ambience for 100min after 5%HF and BHF etching.

Three main absorption peaks are found in the spectrum, and are attributed to absorptions corresponding to SiO stretching ( $\sim 1080\text{cm}^{-1}$ ), SiOH deformation ( $\sim 950\text{cm}^{-1}$ ) or SiO bending ( $\sim 840\text{cm}^{-1}$ ). Intensities of the three peaks as a function of O<sub>2</sub> treatment time are shown for the film etched by BHF in Fig.1. Obvious steplike increases in the absorption intensities may indicate a process of layer-by-layer oxidation. The plateaus in the steplike behavior are seen more clearly and their values are smaller in the sample etched with BHF in comparison to that with 5%HF. It is considered that there are many atomic steps on the Si (111) substrate surface after 5%HF or BHF solution etching. The terraces on the Si surface are well passivated with strong chemical Si-H bonds. Although a part of the Si on the terrace can be oxidized vertical to the substrate surface, it is difficult to oxidize Si on the terrace because of formation of monohydrides. Oxygen can attack reactive sites, such as step edges and dislocations, whose chemical bondings are weak. The nearest neighbor atoms to the oxidized

atom are also attacked easily by oxygen due to the stress. The surface layers of Si parallel to the substrate surface suffer stress from oxidized neighbor atoms and are oxidized more easily than those vertical to the substrate surface. Deeper Si layers require more time for oxidation than shallower layers due to the difficulty of oxygen diffusion. Then, one layer of the substrate surface is oxidized and becomes quasi-stable till oxygen's next attack. A consequent delay in oxidation occurs, and causes the plateaus shown in Fig.1. Moreover, Fig.1 indicates that the plateaus obtained in the surface etched by BHF are longer than those etched by 5%HF; thus, the surface treated by the BHF etching is flatter atomically than that by the 5%HF.

Si wafers were irradiated by UVSOR to study photochemical reaction for hydrogen termination and Si oxidation. Absorption peaks of Si-O( $\sim 1080\text{cm}^{-1}$ ) was not changed by irradiation of UVSOR light in  $\text{O}_2$  or  $\text{H}_2$  ambient. Figure 2 shows spectral change induced by UVSOR irradiation in  $\text{H}_2$  ambient. Si-H absorption on Si( $\sim 2070\text{cm}^{-1}$ ) and Si-H absorption in  $\text{SiO}_2$  film( $\sim 2270\text{cm}^{-1}$ ) increase with increasing irradiation time in  $\text{H}_2$  ambient.  $\text{H}_2$  is dissolved by the UVSOR irradiation and becomes to proton(hydrogen ion). This proton might increase hydrogen terminating Si, and also get into  $\text{SiO}_2$  layer easily.

#### References

- 1) M. Nishida, Y. Matsui, M. Okuyama and Y. Hamakawa: to be published in Jpn. J. Appl. Phys.

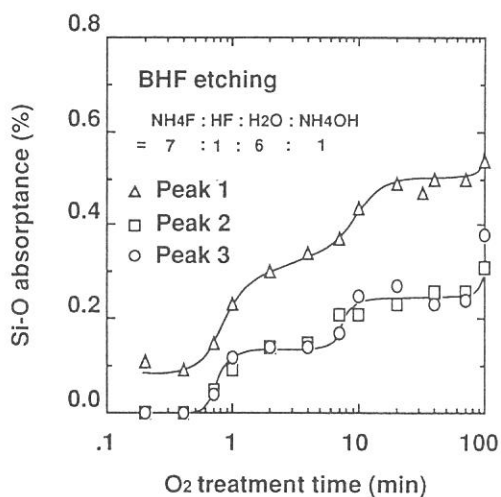


Fig. 1. Intensities of three absorption peaks as a function of oxidation time. Si wafers were etched with BHF. Circles, squares and triangles are absorption intensities at  $\sim 840\text{cm}^{-1}$ ,  $\sim 950\text{cm}^{-1}$  and  $\sim 1080\text{cm}^{-1}$ , respectively.

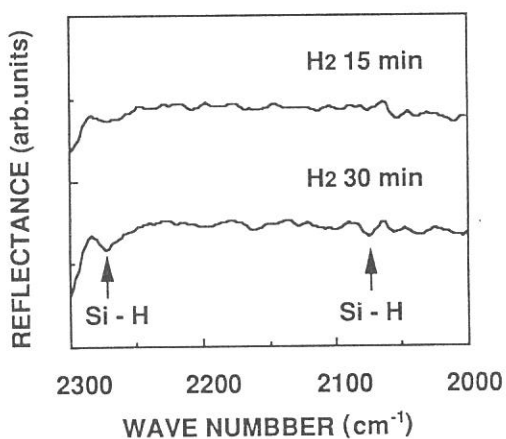


Fig. 2. Relative reflectance spectra of Si surface irradiated in  $\text{H}_2$  ambient for 15 and 30 min by direct light of UVSOR.



# FABRICATION OF SILICON FILMS USING UNDULATOR RADIATION

Masahiro TOMIDA, and Akira YOSHIDA\*

Toyohashi University of Technology, Toyohashi 441

\*Institute for Molecular Science, Okazaki 444

Undulator radiation(UR) emitted from a multipole wiggler is quasi-monochromatic and contains vacuum-ultraviolet light which is suitable to decompose the material gases in semiconductor industry. Therefore, it is a promising light source in photo-CVD(chemical vapor deposition) for future LSI processing. However, there are few reports on photo-CVD utilizing UR. We have fabricated silicon films for the first time using UR as a light source. In this report, the experimental results of UR-CVD of silicon thin films are presented.

## <EXPERIMENTAL>

The experiments were carried out at BL3A1 in UVSOR. The undulator gap was adjusted to 45, 60, and 75 mm :the fundamental lines of photon energy are 19, 36, 50 eV, respectively. The experimental apparatus consists of a differential pumping system that prevents any gases from flowing into the beam line, and of a growth chamber. A nickel mesh was installed 10 mm away over the substrate. Substrates were Si wafers and glass. Disilane gas was introduced to the growth chamber. The flow rate was 2 sccm through a mass flow controller and the growth pressure was kept at 15 mTorr. The substrate temperature was varied from room temperature to 100 °C.

## <RESULTS>

The photograph of the film is shown in Fig. 1. The film was deposited only at the irradiated areas, suggesting that surface reactions are dominant. Moreover, some small fringes were found inside each square. This is due to Fresnel diffraction in which the mesh acts as a slit.

A typical result of Auger electron spectroscopy(AES) is given in Fig. 2. The Si(LVV) peak at 92 eV and Si(KLL) peak at 1619 eV are observed. The contamination due to carbon and oxygen is not found.

Fig. 3 shows the temperature dependence of the growth rate. From this result, the growth rate decreases as the substrate temperature increases: i.e., the activation energy is apparently negative. This fact suggests that the deposition is due to adsorption-controlled process.

Fig. 1. Photograph of silicon film deposited on glass. The substrate temperature was 25°C, and UR gap was 45 mm.

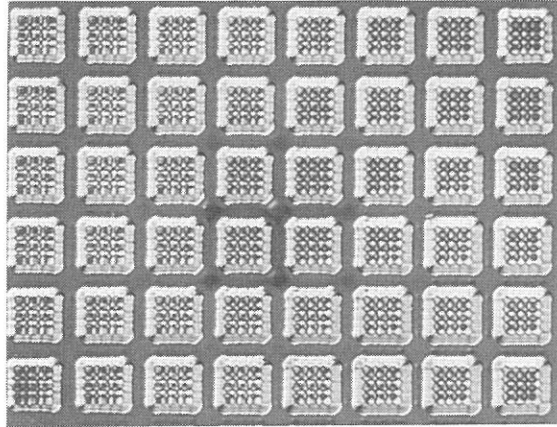


Fig. 2. AES spectra of the specimen deposited on Si at room temperature. UR gap was 60 mm.

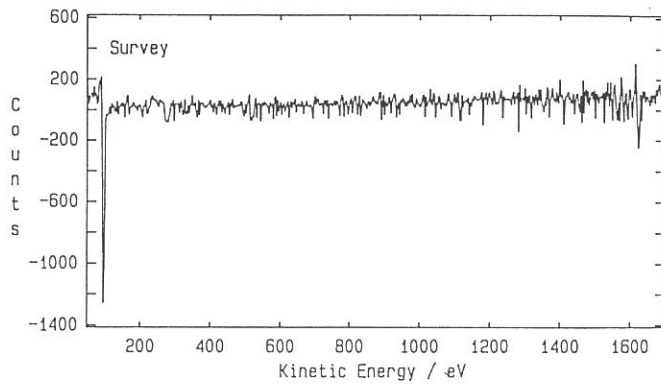


Fig. 3. Substrate temperature dependence of growth rate.

